2-Dimensional Porphyrin Self-Assemblies at Molecular Interfaces

Nicolas Eugster, Koliyat P. Sreenivasan, Bin Su, and Hubert H. Girault*

Laboratoire d'Electrochimie Physique et Analytique, Ecole Polytechnique Fédérale de Lausanne, Station 6, CH-1015 Lausanne, Switzerland

Received September 29, 2005. In Final Form: November 10, 2005

The heterodimer formed by electrostatic association of zinc(II) *meso*-tetrakis(*N*-methylpyridyl)porphyrin (ZnTMPyP) and zinc(II) *meso*-tetrakis(*p*-sulfonatophenyl)porphyrin (ZnTPPS) exhibits a strong affinity for the interface between water and 1,2-dichloroethane (DCE). Surface tension measurements using the quasi-elastic light scattering (QELS) technique reveal that the heterodimer adsorption can be described in terms of a Langmuir isotherm with standard Gibbs energy of adsorption of −45.5 kJ mol^{-1}. The orientation of the heterodimer transition dipole moment, as estimated from light polarization modulated reflectance (LPMR), shows a marked dependence on the bulk concentration of heterodimer. On the other hand, changes in the Galvani potential difference between the two phases have little effect on the heterodimer organization at the water|1,2-dichloroethane interface when the surface coverage is close to maximum. This behavior suggests that the ZnTPPS−ZnTMPyP heterodimer forms an adsorbed layer of aggregated molecules which affects the physical properties of the interface. Indeed, capacitance and surface tension measurements reveal that the dielectric properties of the water|DCE interface are significantly altered in the presence of heterodimer species.

1. Introduction

Interactions between paired porphyrin units have been studied extensively over the past decades.[1] Many of the biologically relevant processes involving porphyrin derivatives, such as photosynthesis, and most porphyrin-based electronic and optical devices are known to depend on interacting porphyrin units. Monitoring the distinctive physicochemical properties of porphyrin dimers not only provides further understanding of biological systems, but is also of crucial interest in any application of multi-porphyrin compounds as molecular receptors.[2]

The quasi co-facial geometry of the "special pair" in the photosynthetic reaction center has led to the investigation of a number of co-facial assemblies of porphyrins or tetrapyrrole compounds. A convenient way of building such a complex is to use ion pair interactions between oppositely charged dyes.[3−18] In such cases, the electrostatic attraction between the charged substituents and the hydrophobic interaction of the aromatic macrocycles cooperate in holding the individual species in close proximity such that extensive orbital overlap can occur. Indeed, porphyrin heterodimers frequently exhibit redox and spectral properties which differ from that of the monomers.[17,18] Recently, the porphyrin heterodimer formed by the association of zinc(II) *meso*-tetrakis(*N*-methylpyridyl)-porphyrin (ZnTMPyP) and zinc(II) *meso*-tetrakis(*p*-sulfonatophenyl)porphyrin (ZnTPPS) has been extensively used as a sensitizer at the water|1,2-dichloroethane boundary, owing to its high affinity for the interfacial region.[19−22] This series of publications offers fundamental insight into the dynamics of heterogeneous electron transfer at molecular interfaces. However, information on the spatial organization of dimer species at the interface is still lacking. In the present contribution, we shall employ quasi-elastic light scattering (QELS) and light polarization modulated reflectance (LPMR) to investigate the adsorption of the ZnTPPS−ZnTMPyP heterodimer as well as that of the free monomers at the water|DCE interface as functions of the bulk concentrations and Galvani potential difference between the two phases.

The interface between two immiscible liquids is generally considered a good model environment for studying heterogeneous reactions and exchange processes occurring in biological systems.[23−25] The advantages provided by this type of system lie in the fact that the interface can be externally polarized and

* To whom correspondence should be addressed. Tel: +41 21 693 3151. Fax: +41 21 693 3667. E-mail: hubert.girault@epfl.ch.

(1) Kadish, K. M.; Smith, K. M.; Guilard, R. *The Porphyrin Handbook*; Academic Press: San Diego, 2000; Vols. 4 and 6.
(2) Pescitelli, G.; Gabriel, S.; Wang, Y.; Fleischhauer, J.; Woody, R. W.; Berova, N. *J. Am. Chem. Soc.* **2003**, *125*, 7613−7628.
(3) Segawa, H.; Nishino, H.; Kamikawa, T.; Honda, K.; Shimidzu, T. *Chem. Lett.* **1989**, 1917.
(4) Tran-Thi, T. H.; Gaspard, S. *Chem. Phys. Lett.* **1988**, *148*, 327.
(5) Tran-Thi, T. H.; Palacin, S.; Clergeot, B. *Chem. Phys. Lett.* **1989**, *157*, 92.
(6) Tran-Thi, T. H.; Lipskier, J. F.; Houde, D.; Pépin, C.; Keszei, E.; Jay-Gerin, J. P. *J. Chem. Soc., Faraday Trans. 2* **1992**, *88*, 2129.
(7) Tran-Thi, T. H.; Lipskier, J. F.; Simoes, M.; Palacin, S. *Thin Solid Films* **1992**, *210, 211*, 150.
(8) Lipskier, J. F.; Tran-Thi, T. H. *Inorg. Chem.* **1993**, *32*, 722.
(9) Tran-Thi, T. H. *Coord. Chem. Rev.* **1997**, *160*, 53.
(10) Ojadi, E.; Selzer, R.; Linschitz, H. *J. Am. Chem. Soc.* **1985**, *107*, 7783.
(11) Gusev, A. V.; Danilov, E. O.; Rodgers, M. A. J. *J. Phys. Chem. A* **2002**, *106*, 1993.
(12) Gusev, A. V.; Rodgers, M. A. J. *J. Phys. Chem. A* **2002**, *106*, 1985.
(13) Hugerat, M.; Levanon, H.; Ojadi, E.; Biczok, L.; Linschitz, H. *Chem. Phys. Lett.* **1991**, *181*, 400.
(14) Springs, S. L.; Gosztola, D.; Wasiliewski, M. R.; Král, V.; Andrievsky, A.; Sessler, J. L. *J. Am. Chem. Soc.* **1999**, *121*, 2281.
(15) Chen, D.-M.; Zhang, Y.-H.; He, T.-J.; Liu, F.-C. *Spectrochim. Acta Part A 2002*, *58*, 2291.
(16) van Willigen, H.; Das, U.; Ojadi, E.; Linschitz, H. *J. Am. Chem. Soc.* **1985**, *107*, 7784.
(17) Hofstra, U.; Koehorst, R. B. M.; Schaafsma, T. J. *Chem. Phys. Lett.* **1986**, *130*, 555.
(18) Vergeldt, F. J.; Koehorst, R. B. M.; Schaafsma, T. J.; Lambry, J. C.; Martin, J. L.; Johnson, D. G.; Wasiliewski, M. R. *Chem. Phys. Lett.* **1991**, *182*, 107.
(19) Fermín, D. J.; Duong, H. D.; Ding, Z.; Brevet, P. F.; Girault, H. H. *J. Am. Chem. Soc.* **1999**, *121*, 10203.
(20) Fermín, D. J.; Lahtinen, R. Dynamic Aspects of Heterogeneous Electron-Transfer Reactions at Liquid|Liquid Interfaces. In *Liquid Interfaces in Chemical, Biological and Pharmaceutical Applications*; Volkov, A. G., Ed.; Marcel Dekker: New York, 2001; Vol. 95, p 179.
(21) Eugster, N.; Fermín, D. J.; Girault, H. H. *J. Phys. Chem. B* **2002**, *106*, 3428.
(22) Eugster, N.; Fermín, D. J.; Girault, H. H. *J. Am. Chem. Soc.* **2003**, *125*, 4862.
(23) Volkov, A. G.; Deamer, D. W. *Liquid−Liquid Interfaces: Theory and Methods*; CRC Press: Boca Raton, FL, 1996.
(24) Volkov, A. G.; Deamer, D. W.; Tanelian, D. I.; Markin, V. S. *Liquid Interfaces in Chemistry and Biology*; John Wiley: New York, 1998.
(25) Reymond, F.; Fermín, D. J.; Lee, H. J.; Girault, H. H. *Electrochim. Acta* **2000**, *45*, 2647.

10.1021/la052642b CCC: $33.50
Published on Web 12/20/2005

that the potential difference between the two phases can be used as a driving force for charge transfer and adsorption phenomena. Koryta et al. first stressed the relevance of adsorbed phospholipid monolayers at liquid|liquid boundaries as a model system for the clarification of biological membrane phenomena.[26] Since then, the formation of monolayers or aggregates at polarized liquid|liquid junctions has been studied employing a variety of experimental techniques.[23,24,27−32] The LPMR technique described in the present paper allows estimation of the average orientation of the transition dipole moment of molecules adsorbed at the interface, which should provide useful information on how adsorbates arrange themselves at molecular interfaces. Indeed, our measurements reveal that the organization of the ZnTPPS−ZnTMPyP heterodimer at the water|DCE interface is dependent on its bulk concentration as well as on the potential difference between the two phases. At a bulk concentration of 10^{-4} mol dm^{-3} in the aqueous phase, the surface coverage approaches its maximum and the organization of the heterodimer becomes practically independent of the applied potential.

2. Experimental Section

All reagents employed were analytical grade. Water was purified using a Milli-Qplus 185 Millipore installation. Zinc(II) *meso*-tetrakis-(*N*-methylpyridyl)porphyrin (ZnTMPyP) and zinc(II) *meso*-tetrakis-(*p*-sulfonatophenyl)porphyrin (ZnTPPS) were employed as received from Frontier Scientific. The organic electrolyte bis(triphenyl-phosphoranylidene)ammonium tetrakis(pentafluoro-phenyl)borate (BTPPATPFB) was prepared by metathesis of BTPPACl (Fluka) and LiTPFB (Boulder Scientific) in 2:1 mixtures of methanol and water, followed by recrystallization in acetone.[33]

The experimental QELS setup is depicted in Figure 1a. The beam from a 4 mW He−Ne laser at 632.8 nm (Uniphase model 1101) passes through the bottom of the four-electrode glass cell (area 1.53 cm^2) and illuminates the interface perpendicularly. The water surface was covered with an optical glass window to minimize the light scattering from the air|water interface. A diffraction grating consisting of dark lines on a photographic glass plate was placed after the optical cell. An optical beat was generated by mixing the diffracted light with the light scattered by the capillary waves at the liquid|liquid interface. The beat corresponding to the third-order diffraction spot was monitored by a photomultiplier tube and analyzed using a Stanford Research Systems SR770 fast-Fourier transform analyzer.

The LPMR setup is schematically represented in Figure 1b. The 442 nm beam from a He−Ne laser (OmNichrome S74) first passes through a polarizer and then the optical element of the photoelastic modulator (Hinds Instruments PEM-90). The PEM introduces a periodical retardation in the component of the electric field along the modulator axis.[34,35] When the retardation maximum is set to half the wavelength of the laser light and the difference between the angles α and β (Figure 1c) is equal to 45°, the polarization of the light beam at the liquid|liquid interface varies periodically between

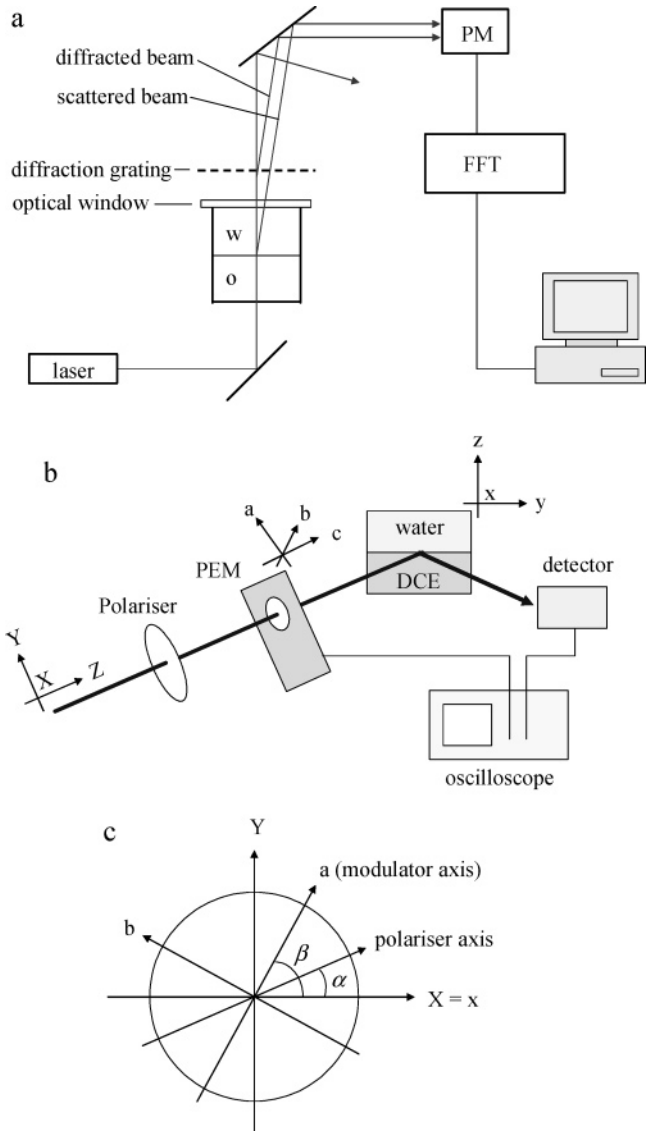

Figure 1. (a) Schematic diagram of the QELS setup. (b) Schematic diagram of the polarization modulated reflectance setup. (c) Schematic representation of the angles α and β. The direction of propagation of the laser beam is perpendicular to *X* and *Y*. The axis "*a*" is the modulation axis of the PEM.

parallel and perpendicular. The beam reaches the interface with an angle χ of 72°, ensuring total internal reflection conditions. The reflected beam is collected by an optical fiber to a photomultiplier tube. The signal from the detector contains a modulation at the frequency of the PEM.

Homemade glass cells with built-in luggin capillaries and platinum counter electrodes were used in QELS, LPMR, and capacitance measurements. No supporting electrolytes were added to the liquid phases in the absence of applied potential. When working under potentiostatic conditions, the following electrochemical cell was employed:

$$Ag|Ag_2SO_4|Li_2SO_4,\ \text{porphyrins (w)}||\text{BTPPATPFB (o)}|\text{BTPPACl, LiCl (w)}|AgCl|Ag$$

with the concentrations of Li_2SO_4, BTPPATPFB, BTPPACl and LiCl being 10^{-2}, 5×10^{-3}, 10^{-3} and 10^{-2} mol dm^{-3} respectively. The double line represents the polarized liquid|liquid interface, and (w) and (o) denote aqueous and organic phases, respectively. The potential was controlled via a custom-built 4-electrodes potentiostat.[30] The Galvani potential difference was estimated from the formal transfer potential of tetramethylammonium (0.160 V). The differential

(26) Koryta, J.; Hung, L. W.; Hofmanová, A. *Studia Biophys.* **1982**, *90*, 25.
(27) Girault, H. H.; Schiffrin, D. J. Electrochemistry of Liquid−Liquid Interfaces. In *Electroanalytical Chemistry*; Bard, A. J., Eds.; Dekker: New York, 1989; Vol. 15, p 1.
(28) Girault, H. H. Charge Transfer across Liquid−Liquid Interfaces. In *Modern Aspects of Electrochemistry*; Bockris, J. O. M., Conway, B., White, R., Eds.; Plenum Press: New York, 1993; Vol. 25, p 1.
(29) Kakiuchi, T. Adsorption at Polarized Liquid−Liquid Interfaces. In *Liquid Interfaces in Chemical, Biological and Pharmaceutical Applications*; Volkov, A. G., Ed.; Marcel Dekker: New York, 2001; Vol. 95, p 105.
(30) Samec, Z. *Chem. Rev.* **1988**, *88*, 617.
(31) Senda, M.; Kakiuchi, T.; Osakai, T. *Electrochim. Acta* **1991**, *36*, 253.
(32) Samec, Z.; Kakiuchi, T. Charge-Transfer Kinetics at Water-Organic Solvent Phase Boundaries. In *Advances in Electrochemical Science and Engineering*; Gerischer, H., Tobias, C. W., Eds.; VCH: Weinheim, Germany, 1995; Vol. 4, p 297.
(33) Fermín, D. J.; Duong, H. D.; Ding, Z.; Brevet, P. F.; Girault, H. H. *Phys. Chem. Chem. Phys.* **1999**, *1*, 1461.
(34) Jasperson, S. N.; Schnatterly, S. E. *Rev. Sci. Instr.* **1969**, *40*, 761.
(35) Hipps, K. W.; Crosby, G. A. *J. Phys. Chem.* **1979**, *83*, 555.

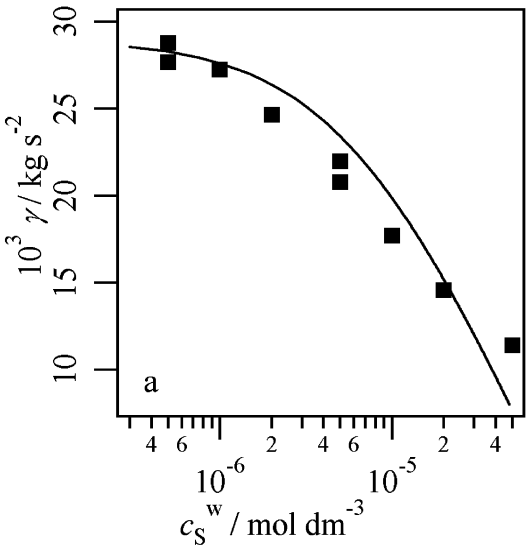

Figure 2. Surface tension of the water|DCE interface as a function of the bulk concentration of ZnTPPS−ZnTMPyP heterodimer, in the absence of supporting electrolytes. The solid line is a fitting using eq 7 with the parameters $\gamma_0 = 0.029$ kg s^{-2}, $\Gamma_S^{max} = 4 \times 10^{-6}$ mol m^{-2}, and $\Delta G_{ads} = -45.5$ kJ mol^{-1}.

capacitance was estimated from admittance measurements at 12 Hz with amplitude of 4 mV rms.

3. Results and Discussion

3.1. Adsorption of the ZnTMPyP−ZnTPPS Heterodimer as a Function of the Aqueous Concentration. The specific adsorption of the ZnTPPS−ZnTMPyP heterodimer at the water|DCE interface can be followed by changes in the interfacial surface tension. The QELS method allows for estimation of the surface tension γ from the characteristic frequency of the thermally activated capillary waves. The relation between these two parameters is given by Lamb's equation,[36] as described in Appendix A.

Figure 2 shows the evolution of the water|DCE surface tension as a function of the concentration of heterodimer in the absence of supporting electrolyte. To a first approximation, we shall assume that the surface coverage can be related to the bulk concentration in terms of a Langmuir isotherm. Thus, the surface tension as a function of bulk concentration can be described by eq 1, with the maximum surface concentration Γ_S^{max} and the Gibbs energy of adsorption ΔG_{ads} as adjustable parameters (see Appendix A).

$$\gamma = \gamma_0 - \Gamma_S^{max} RT \ln\left(1 + \frac{c_S^w}{c_w^w} \exp\left(\frac{-\Delta G_{ads}}{RT}\right)\right) \qquad (1)$$

The term γ_0 denotes the surface tension in the absence of porphyrins, c_S^w is the bulk concentration of heterodimer, and c_w^w is the concentration of water molecules in water, i.e., 55.5 mol dm^{-3}. The solid line in Figure 2 illustrates the fit of eq 1 to the experimental data. The Gibbs energy of adsorption (ΔG_{ads}) associated with the heterodimer is evaluated as -45.5 kJ mol^{-1}, which is considerably larger than the values obtained from photocurrent measurements or second harmonic generation in the case of various porphyrin monomers.[37−40] The fact that the experimental data can be described with a constant value of ΔG_{ads} indicates that the Langmuir isotherm is a reasonable approximation for the heterodimer adsorption. According to the parameters obtained from the fit in Figure 2, more than 96% of the maximum coverage is attained with a bulk concentration of 2×10^{-5} mol dm^{-3}. The maximum surface concentration is estimated to be 4×10^{-10} mol cm^{-2}, which corresponds to a surface area of about 0.4 nm^2 per porphyrin complex. This high surface density indicates that a film of aggregated porphyrins is formed at the interface. As discussed later, this 2-dimensional porphyrin structure is determining to the properties of the liquid|liquid interface.

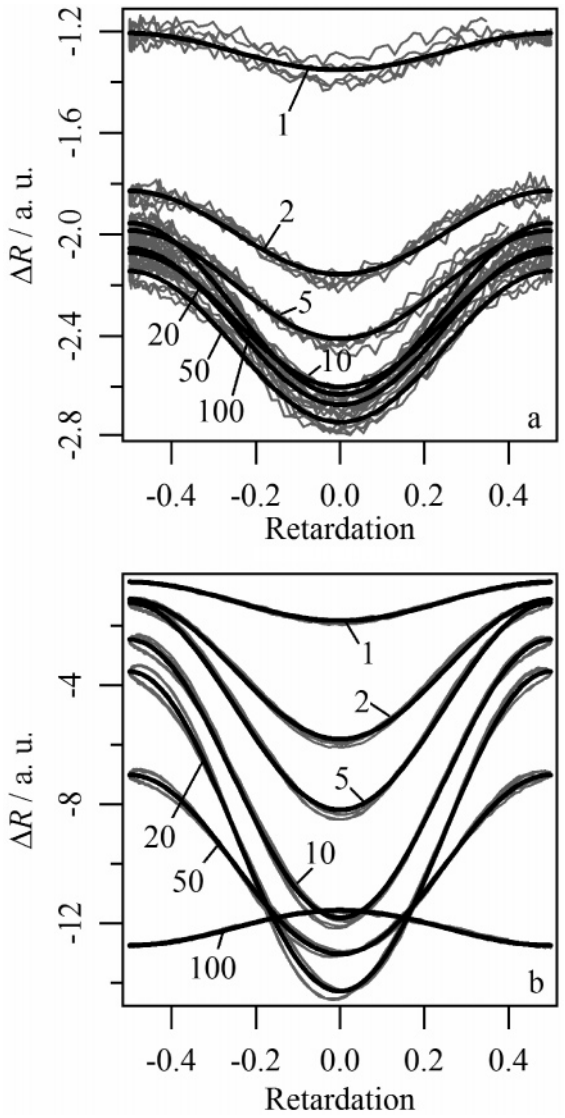

Figure 3. Reflectance signal as a function of the wave retardation in the presence of ZnTPPS (a) or ZnTPPS−ZnTMPyP heterodimer (b) in the aqueous phase. Bulk concentrations are indicated on the graphs in μmol dm^{-3}. The solid lines are fits of eq 21 to the experimental data, taking C and ξ as adjustable parameters.

Figure 3 displays typical LPMR curves measured with the setup described in Figure 1b in the presence of ZnTPPS (a) or the ZnTPPS−ZnTMPyP heterodimer (b) in the aqueous phase. The detected signal is displayed as a function of the retardation in relative units. A retardation of 0.5 means that the polarization

(36) Lamb, H. *Hydrodynamics*; Dover: New York, 1945.
(37) Fermín, D. J.; Ding, Z.; Duong, H. D.; Brevet, P. F.; Girault, H. H. *J. Phys. Chem. B* **1998**, *102*, 10334.
(38) Jensen, H.; Fermin, D. J.; Girault, H. H. *Phys. Chem. Chem. Phys.* **2001**, *3*, 2503.
(39) Nagatani, H.; Fermin, D. J.; Girault, H. H. *J. Phys. Chem. B* **2001**, *105*, 9463.
(40) Nagatani, H.; Piron, A.; Brevet, P. F.; Fermín, D. J.; Girault, H. H. *Langmuir* **2002**, *18*, 6647.

component parallel to the modulator axis leads the perpendicular component by half the value of the beam wavelength. Providing that the angle between the initial polarization and the modulator axis ($\beta-\alpha$ in Figure 1c) is equal to 45°, the beam at this point is linearly polarized at 90° with respect to the initial polarization (retardation = 0). The setup in Figure 1b is disposed in such a way that the laser beam reaches the liquid|liquid interface with polarization parallel to the interfacial plane. Therefore, retardation values of 0 and ±0.5 correspond to parallel and perpendicular polarization, respectively. At other retardation values the beam is circularly polarized.

The data in Figure 3a reflect the increase in surface concentration of ZnTPPS as the bulk concentration is increased. The relatively small changes in the curvature of the response indicate that the orientation of the ZnTPPS molecules does not vary much as the surface coverage increases. This situation can be contrasted to the case of the ZnTPPS−ZnTMPyP heterodimer, where pronounced changes in both the amplitude and shape of the response are observed. The data in Figure 3b suggest that the organization of the dimer at the interface is largely influenced by the bulk concentration of porphyrins. In principle, the signal measured in Figure 3b corresponds to the absorption of light by dimer species as well as monomers. However, the association constant between ZnTPPS and ZnTMPyP in similar conditions has been reported to be larger than 10^7 mol^{-1} dm^3.[19] In the following discussion, the reflectance associated with remaining monomers at the interface will be neglected whenever both porphyrins are present in solution.

To quantitatively analyze these results, it is necessary to describe how the modulated electric field at the interface interacts with the transition dipole moment of the adsorbed species. The development presented in Appendix B is based on several assumptions: (i) The reflection plane is supposed to coincide with the adsorption plane of the dyes. (ii) The light absorption by porphyrins in the bulk is not considered. Indeed, photocurrent measurements under total internal reflection conditions as functions of the incoming angle of the illumination beam using similar porphyrins have shown that this assumption is reasonable.[38,41,42] (iii) The porphyrin molecules exhibit an average orientation with respect to the interfacial plane (x,y) (see Figure 1b), but can rotate freely around the axis (z) perpendicular to the interface. (iv) Finally, although porphyrins are known to exhibit two orthogonal transition dipoles located in the plane of the ring,[43] we shall consider the interaction of the electric field with a single dipole moment for all adsorbed species. As described in Appendix B, the reflectance at a given value of the retardation is a function of the orientation angle ξ and depends on several geometrical parameters of the setup

$$\Delta R = \frac{I - I_0}{I_0} = f(C,\xi) \qquad (2)$$

where I and I_0 correspond to the detector signal in the presence and in the absence of porphyrins, respectively. The angle ξ is defined as the angle between the interfacial plane and the transition dipole, as shown in Figure 4. The angle φ in this figure describes the orientation of the transition dipole on the plane of the interface, which is considered to be random. The parameter C describes the modulation amplitude of the detected signal. This term regroups the light intensity, the density of transition dipoles, and the characteristics of the detector. Under controlled experimental conditions, C is proportional to the surface concentration of adsorbate.

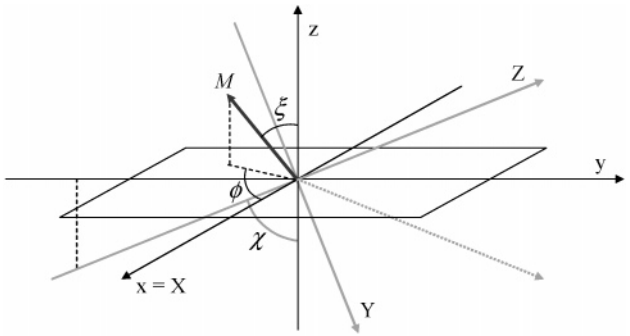

Figure 4. Scheme of the incident and reflected beams at the interface under total internal reflection. The interface is defined as the (x,y) plane. The incident beam travels along the Z direction, which is at an angle χ to the axis z perpendicular to the interface. The transition dipole moment M is defined by the angles ξ and φ.

The dark lines in Figure 3 are fits of the experimental data to the theoretical expression developed in Appendix B. The adjustable parameters C and ξ are displayed as functions of the bulk concentration of the corresponding species in Figure 5. The solid line in Figure 5a is proportional to the Langmuir isotherm inferred from the QELS measurements in Figure 2. The smaller signals obtained in the presence of the ZnTPPS or ZnTMPyP monomers reflect the charge repulsion between adsorbates, which prevents the formation of closely packed layers at the interface. The two experiments provide a consistent picture of the evolution of the ZnTPPS−ZnTMPyP heterodimer concentration at the water|DCE interface. The Langmuir model appears appropriate, although it seems improbable that no interactions occur between heterodimer species.

The evolution of the orientation angle ξ of the transition dipole moment (Figure 5b) offers further insight into inter-porphyrin interactions at the interface. In the case of the monomers, the angle ξ shows very little variation when the bulk concentration is increased, despite the larger number of adsorbed molecules. This behavior can be contrasted to the case of *meso*-tetrakis-(*p*-carboxyphenyl)porphyrin (ZnTPPC),[41] where hydrogen bonding between the adsorbates results in marked changes in the orientation angle. Similarly to ZnTPPC, large variations of ξ are observed in the presence of the heterodimer.

Interpretation of these results requires knowledge of the nature of transition dipoles in the ZnTPPS−ZnTMPyP heterodimer. Ultrafast time-resolved spectroscopy measurements have shown that the dimer undergoes interporphyrin electron transfer within 100 ps after excitation.[22] This electronic rearrangement leads to a charge transfer state of the form [(ZnTMPyP)$^{3+}$(ZnTPPS)$^{3-}$] with a lifetime extending into the microsecond range. At short times after illumination, the transient absorption spectra of excited porphyrin dimers is roughly the sum of those of the two monomers.[44] Therefore, we can reasonably assume that the dimer photoexcitation proceeds via the excitation of a paired monomer followed by relaxation to the charge transfer state. In the following discussion, the transition dipole is taken to be in the plane of one of the monomers. Considering that the porphyrins feature face-to-face conformation,[15,22] the transition dipole is perpendicular to the center-to-center axis of the dimer. According to Figure 5b, the ZnTPPS−ZnTMPyP dimer adopts an orientation nearly

(41) Jensen, H.; Kakkassery, J. J.; Nagatani, H.; Fermín, D. J.; Girault, H. H. *J. Am. Chem. Soc.* **2000**, *122*, 10943.

(42) Eugster, N.; Jensen, H.; Fermín, D. J.; Girault, H. H. *J. Electroanal. Chem.* **2003**, *560*, 143.

(43) Gouterman, M. *The Porphyrins*; Academic Press: New York, 1978; Vol. 3.

(44) Eugster, N. Dynamic Photoelectrochemistry at Porphyrin-Sensitised Liquid|Liquid Interfaces, EPFL, 2004.

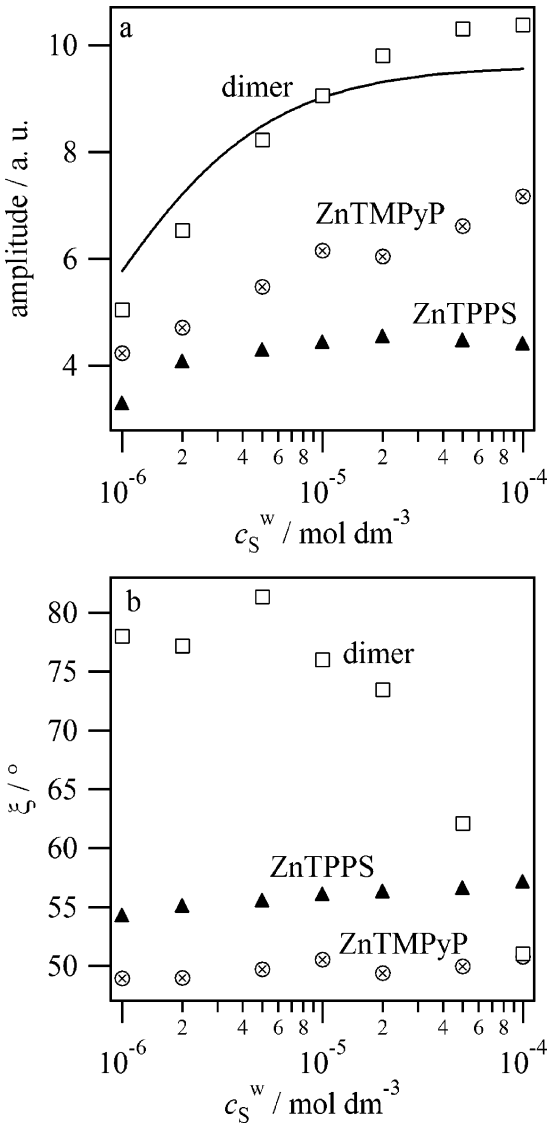

Figure 5. Modulation amplitude C of the reflectance signal (a) and orientation angle ξ (b) as functions of the bulk concentration c_S^w of ZnTPPS, ZnTMPyP, or heterodimer, as extracted from the data in Figure 3.

perpendicular to the axis z at relatively low concentrations. The porphyrin rings lie flat on the interface, suggesting that at incomplete coverage the orientation of the dimer in the absence of applied potential is controlled by the solubility of the paired dyes. When the surface coverage of the heterodimer approaches its maximum, the angle ξ decreases to values close to what is observed in the case of the monomers. As shall be discussed in the following section, the orientation at high surface concentrations is determined by the formation of a film of aggregated porphyrins at the interface.

3.2. Adsorption as a Function of the Galvani Potential Difference between the Two Phases. As mentioned in the Introduction, the ZnTPPS−ZnTMPyP heterodimer has been extensively used as a sensitizer for photocurrent generation at the liquid|liquid interfaces. These studies have allowed characterization of the dependence of the rate of electron transfer on the Galvani potential difference $\Delta_o^w\phi$ between the two immiscible liquids. The analysis of the photocurrent responses was based on the assumption that the surface concentration of dimer remains independent of the potential.[21,22] Such a behavior appears reasonable considering that the dimer forms an overall neutral entity. Furthermore, surface concentration isotherms inferred

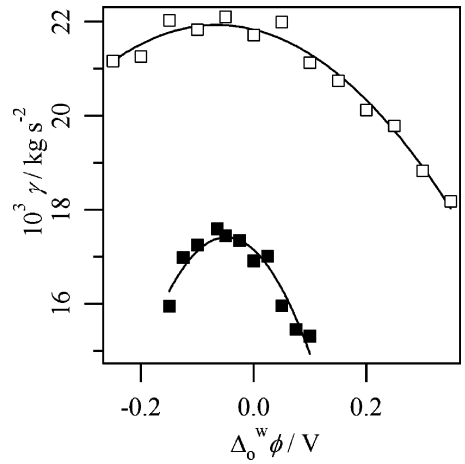

Figure 6. Electrocapillary curves measured by QELS in the absence (white squares) and in the presence of 10^{-4} mol dm^{-3} of ZnTMPyP−ZnTPPS heterodimer (black squares). The aqueous phase contained 10^{-2} mol dm^{-3} Li_2SO_4, whereas the DCE phase contained 5×10^{-3} mol dm^{-3} BTPPATPFB.

from photocurrent measurements have shown that the energy of adsorption does not vary with the applied potential.[19] Here we shall support these observations employing QELS, capacitance, and LPMR measurements.

Figure 6 shows the evolution of the surface tension measured with the QELS technique as a function of the applied potential. Open squares correspond to the bare water|DCE interface, while the solid squares were obtained in the presence of 10^{-4} mol dm^{-3} of ZnTPPS and 10^{-4} mol dm^{-3} of ZnTMPyP in the aqueous phase. The supporting electrolytes Li_2SO_4 and BTPPATPFB were present in the aqueous and organic phases, respectively. These salts are responsible for the lower surface tension observed here compared to the case of Figure 2. The potential corresponding to the maximum of the electrocapillary curve (E_{max}) appears unaffected by the presence of heterodimer, although the surface tension is substantially decreased. E_{max} is commonly referred to as the potential of zero charge, i.e., the potential in which the charge of the diffuse layer on each side of the interface is zero. The results in Figure 6 confirm that the potential difference between the two phases has little effect on the surface coverage of the heterodimer, as the surface tension decreases symmetrically around E_0.

The specific adsorption of ionic species at the liquid|liquid boundary also manifests itself by perturbations of the differential capacitance, as illustrated by Figure 7. The symmetrical potential dependence of the capacitance around the potential of zero charge for the water|DCE junction is strongly affected in the presence of the charged monomers. In the case of ZnTPPS, the minimum of the capacitance shifts to positive potentials, showing a steep increment of the capacitance toward negative potentials. This behavior is consistent with the specific adsorption of hydrophilic anionic species featuring a strong affinity for the liquid|liquid boundary.[42,45] In the case of ZnTMPyP, the minimum of the capacitance curve shifts toward more negative potentials due to the positive charge on the dye. On the other hand, substantial changes to the capacitance−potential curves are observed when both ZnTPPS and ZnTMPyP are present in the aqueous phase. The minimum of the capacitance is observed at negative potentials. The potential dependence appears somewhat weakened, suggesting a change in the interfacial relative permittivity. These phenomena have been observed during the formation of a dense

(45) Su, B.; Eugster, N.; Girault, H. H. *J. Electroanal. Chem.* **2005**, *577*, 187.

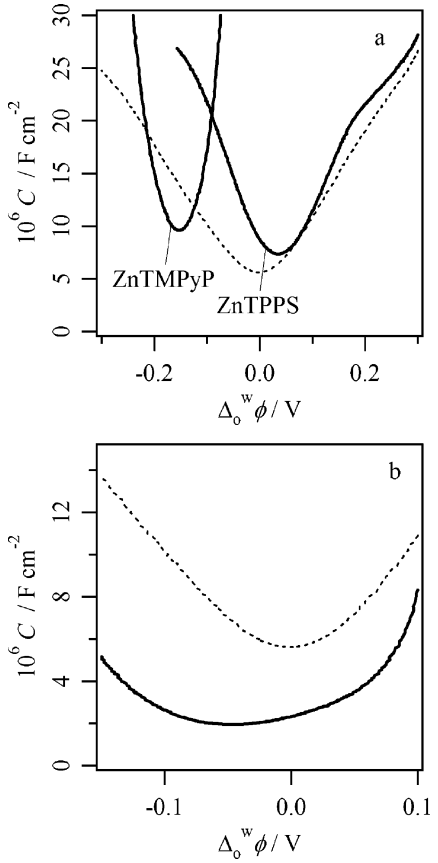

Figure 7. Differential capacitance-potential curves of the water|DCE interface in the presence of ZnTMPyP 10^{-4} mol dm^{-3} or ZnTPPS 10^{-4} mol dm^{-3} (a) or 10^{-4} mol dm^{-3} of both porphyrins (b). The dotted line corresponds to the capacitance in the absence of dye species. The aqueous phase contained 10^{-2} mol dm^{-3} Li_2SO_4, whereas the DCE phase contained 5×10^{-3} mol dm^{-3} BTPPATPFB.

neutral surfactant-type monolayer at the liquid|liquid boundary.[30,42] The minimum of the capacitance curve appears much decreased in comparison with the blank capacitance. This behavior is consistent with the insertion of a low-permittivity dielectric material at the interface. It could be envisaged that the heterodimer aggregates at the interface but retains a high polarizability due to the delocalization of the electrons. Hence, the charge on one side of the interface is less screened in the presence of ZnTMPyP−ZnTPPS aggregates, resulting in a lower capacitance. These results can be compared to the QELS measurements in Figure 6. Both sets of data suggest that the adsorption of a layer of heterodimer species strongly affects the physicochemical properties of the water|DCE interface.

Figure 8 displays light polarization modulated reflectance curves in the presence of 10^{-4} mol dm^{-3} ZnTPPS in the aqueous phase at various potential differences. The black lines are fits to the experimental data (in gray) employing the equation derived in Appendix B. It can be observed that the amplitude of the response increases when the potential is tuned to more negative values, reflecting the increase in the ZnTPPS surface concentration. At very negative potentials, the amplitude of the oscillation decreases while the overall reflectance magnitude is larger, revealing a change in the orientation of the transition dipoles at the interface. This is clearly visible in Figure 9, which displays the amplitude C and the orientation angle ξ as functions of the potential for the three porphyrin species. The values of C and ξ were extracted from the fit to the experimental data shown in Figure 8. The dashed lines correspond to the formal ion transfer potentials of ZnTPPS ($\Delta_o^w\phi^{o\prime}_{ZnTPPS} = -0.29$ V) and ZnTMPyP

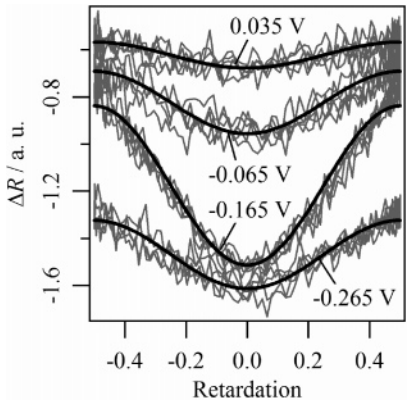

Figure 8. Reflectance signal as a function of the wave retardation in the presence of ZnTPPS at various Galvani potential differences. The solid lines are fits of the experimental data to eq 21, taking C and ξ as adjustable parameters. The aqueous phase contained 10^{-2} mol dm^{-3} Li_2SO_4, whereas the DCE phase contained 5×10^{-3} mol dm^{-3} BTPPATPFB.

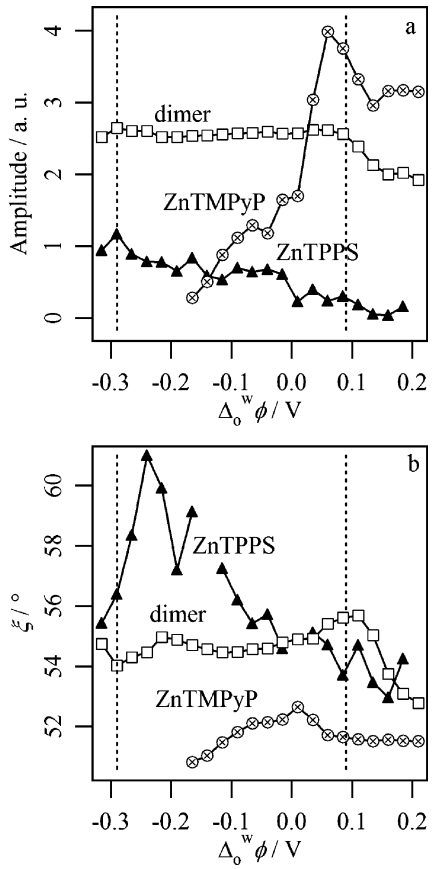

Figure 9. Modulation amplitude C of the reflectance signal (a) and orientation angle ξ (b) as functions of the Galvani potential difference in the presence of 10^{-4} mol dm^{-3} ZnTPPS, ZnTMPyP, or heterodimer, as extracted from the data in Figure 7.

($\Delta_o^w\phi^{o\prime}_{ZnTMPyP} = 0.09$ V).[19] The concentration of the charged monomers increases when approaching the transfer potential, reflecting the higher surface excess charge observed by capacitance measurements in Figure 7. On the other hand, the amplitude of the modulated reflectance in the presence of the ZnTPPS−ZnTMPyP heterodimer appears unaffected by the changes in the Galvani potential difference. This result confirms again that the surface concentration of heterodimer remains constant throughout the potential window delimited by the formal ion transfer potentials of the monomers.

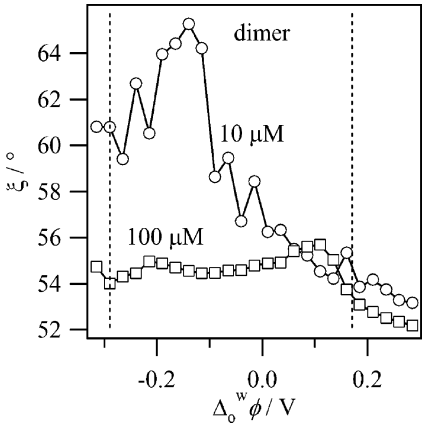

Figure 10. Orientation angle ξ as a function of the Galvani potential difference in the presence of 10^{-4} mol dm^{-3} and 10^{-5} mol dm^{-3} heterodimer.

The orientation angle of the heterodimer in 10^{-4} mol dm^{-3} concentration also appears to have very little dependence on the potential difference between the two phases, although some variations are observed (see Figure 9b). It should be noticed that, even at potentials close to the transfer of ZnTMPyP, the dimer remains oriented with an angle of about 55° with respect to the normal to the interface. This situation can be contrasted to the case of the two monomers, where the angle ξ increases at potentials close to the transfer potential, particularly in the presence in the case of ZnTPPS where changes of about 8° are observed. The dependence of the angle ξ on the potential in the cases of ZnTPPS and ZnTMPyP monomers differs from earlier results obtained with ZnTPPC.[41] In the presence of ZnTPPC, the porphyrin rings adopt a more upward position at high surface coverage to accommodate more molecules. However, it has been shown that hydrogen bonding involving the carboxylic groups of ZnTPPC plays a large role in its adsorption at the water|DCE interface.

An intriguing observation is that the orientation of the ZnTPPS−ZnTMPyP heterodimer varies a lot with the Galvani potential difference when the surface coverage is far from complete, as shown in Figure 10. Although the signal amplitude observed with a heterodimer bulk concentration of 10^{-5} mol dm^{-3} did not show any significant changes between −0.29 and +0.09 V, the angle ξ exhibits a marked dependence on the potential. At low surface coverage, the dimer species are free to rotate and adapt to the potential distribution, thereby adopting a position in which the porphyrin rings lie nearly in the plane of the liquid|liquid interface.

Finally, the following picture emerges for the adsorption of the ZnTPPS−ZnTMPyP heterodimer at the water|DCE interface: at relatively low bulk concentrations (below 10^{-5} mol dm^{-3}), interactions between adsorbates are negligible and the surface coverage can be rationalized in terms of a Langmuir isotherm. Adsorbed heterodimer species are free to rotate in order to adapt to the potential distribution across the interface. When the potential difference between the two phases approaches the transfer potential of ZnTPPS, the heterodimer adopts a position in which the porphyrin rings are nearly in the plane of the interface. However, if the bulk concentration is increased and the surface coverage approaches saturation, the heterodimer species arrange themselves at the liquid|liquid boundary with fixed orientation angle and surface concentration. Within the limits imposed by the transfer of porphyrins to the organic phase, the potential has little effect on the heterodimer adsorption, as the interactions between heterodimer units overcome their ability to follow the imposed electric field. These interactions result in the formation of an aggregated, ordered layer which strongly affects the dielectric properties of the interface.

4. Conclusions

The self-organization of the water-soluble porphyrin heterodimer ZnTPPS−ZnTMPyP at the water|DCE interface was investigated employing various techniques. QELS and LPMR measurements reveal that the dependence of the surface concentration of heterodimer on the bulk concentration in water can be rationalized in terms of a Langmuir isotherm. This treatment yields a Gibbs energy of adsorption of −45.5 kJ mol^{-1}. Analysis of the LPMR data also allows extracting information of the average orientation of the dipole transition moments at the interface. Although the orientation of the ZnTPPS and ZnTMPyP monomers appears weakly dependent on the bulk concentration of porphyrins, the ZnTPPS−ZnTMPyP exhibits large variations of the orientation angle. At low surface coverage, the porphyrin rings of the heterodimer species are nearly in the plane of the interface. At surface concentrations close to saturation, the heterodimer organization is controlled by aggregation phenomena, resulting in an average angle of 55° between the transition dipole and the normal to the interface.

Capacitance, QELS, and LPMR measurements as functions of the Galvani potential difference show that the heterodimer organization at a large surface coverage is practically potential independent. Although in the case of the monomers the surface concentration increases sharply near their ion transfer potentials, the heterodimer shows a constant surface concentration throughout the potential window. The orientation of the porphyrin rings also remains stable when the potential is varied, again indicating that the aggregation determines the orientation. Finally, capacitance and electrocapillary curves suggest that the heterodimer species form a compact layer of aggregates at the liquid|liquid boundary, thereby changing the dielectric properties of the interface.

Acknowledgment. This work was supported by the Fond National Suisse de la Recherche Scientifique (Project 20-67050.01). The technical assistance by Valérie Devaud is acknowledged.

Appendix A: Interpretation of the QELS Results

The QELS method monitors the frequencies of thermally activated capillary waves, which can be related to the interfacial surface tension using Lamb's equation[36]

$$f_0 = \frac{1}{2\pi}\left(\frac{\gamma}{\rho_w + \rho_o}\right)^{1/2} k^{3/2} \tag{3}$$

where f_0 is a characteristic frequency of the capillary waves and ρ_w and ρ_o are the densities of the aqueous and organic solvents, respectively. The circular wavenumber k of the capillary wave is associated to that of the incident beam (K) according to eq 4

$$K \tan(\theta) = k \tag{4}$$

The angle θ is fixed by using a grating of constant d and choosing the order of diffraction

$$d \sin(\theta) = n\lambda \tag{5}$$

where n is the order of diffraction and λ is the wavelength of the laser beam ($\lambda = 2\pi/K$). In practice, the angle θ is sufficiently small to allow the approximation that $\sin(\theta) = \tan(\theta) = \theta$, therefore

$$k = \frac{2\pi n}{d} \tag{6}$$

The slit width d was estimated as 0.335 mm by measuring the diffraction angle of the tenth order spot. The wavenumber associated with the third order diffraction can be readily estimated at $k = 563\ \mathrm{cm}^{-1}$ from eq 6.

The surface concentration of ZnTPPS−ZnTMPyP heterodimer can be calculated from the Gibbs surface tension equation

$$\Gamma_S = -\frac{1}{RT}\frac{d\gamma}{d\ln(c_S^w)} \tag{7}$$

where c_S^w is the bulk concentration of heterodimer. To a first approximation, the surface coverage can be described in terms of a Langmuir isotherm[29,45]

$$\Gamma_S = \Gamma_S^{max}\frac{\frac{c_S^w}{c_w^w}\exp\left(-\frac{\Delta G_{ads}}{RT}\right)}{1+\frac{c_S^w}{c_w^w}\exp\left(-\frac{\Delta G_{ads}}{RT}\right)} \tag{8}$$

where c_w^w is the concentration of water molecules in water, i.e., 55.5 mol dm^{-3}. Combining eqs 7 and 8 yields eq 1 after integration.

Appendix B: Reflectance as a Function of the Retardation

The coordinates (X,Y,Z), (a,b,c), and (x,y,z), corresponding to the laser beam, the PEM, and the liquid|liquid interface, respectively, are shown in Figure 1b. The field of the laser beam after passing through the polarizer can be represented in the referential (a,b,c) of the PEM as

$$E_1 = \begin{pmatrix} E_0\cos\alpha \\ E_0\sin\alpha \\ 0 \end{pmatrix}_{XYZ} = \begin{pmatrix} A \\ B \\ 0 \end{pmatrix}_{abc} \tag{9}$$

where

$$A = E_0(\cos\alpha\cos\beta + \sin\alpha\sin\beta) \tag{10}$$

and

$$B = E_0(\sin\alpha\cos\beta - \cos\alpha\sin\beta) \tag{11}$$

The term E_0 corresponds to the magnitude of the initial electric field, α is the angle of the initial polarization of the beam, and β describes the orientation of the modulator axis (see Figure 1c). When passing through the PEM, the field component with polarization along the modulator axis is periodically retarded with respect to the component perpendicular to the modulator axis[34,35]

$$E_2 = \begin{pmatrix} A\exp(i\phi) \\ B \\ 0 \end{pmatrix}_{abc} = \begin{pmatrix} A\exp(i\phi)\cos\beta - B\sin\beta \\ -A\exp(i\phi)\sin\beta\cos\chi - B\cos\beta\cos\chi \\ A\exp(i\phi)\sin\beta\sin\chi + B\cos\beta\sin\chi \end{pmatrix}_{xyz} \tag{12}$$

where χ is the angle between the incoming beam (axis Z) and the normal to the interface (axis z). The parameter ϕ denotes the phase difference between the components at any time.

$$\phi = \phi_0\cos(\omega t) \tag{13}$$

The maximum phase shift ϕ_0 induced in the light beam during a period of the modulator oscillation is a function of the light wavelength and the maximum voltage applied to the modulator.[35] For all measurements in this paper, these parameters were set so that $\phi_0 = \pi$ (i.e., the maximum retardation is equal to 0.5). The field of the reflected beam can be calculated using the Fresnel equations

$$\left(\frac{E_r}{E_i}\right)_{||} = \frac{n^o\cos\chi - n^w\cos\theta}{n^o\cos\chi + n^w\cos\theta} = r_{||} \tag{14}$$

$$\left(\frac{E_r}{E_i}\right)_{\perp} = \frac{n^o\cos\theta - n^w\cos\chi}{n^o\cos\theta + n^w\cos\chi} = r_{\perp} \tag{15}$$

where n^o and n^w denote the refraction index of DCE (1.445) and water (1.333), respectively. The angle θ is the refraction angle, which is imaginary under total internal reflection conditions. This angle is obtained from Snell's law

$$n^o\sin\chi = n^w\sin\theta \tag{16}$$

which yields

$$\cos\theta = i\left(\left(\frac{n^o}{n^w}\right)^2\sin^2\chi - 1\right)^{1/2} \tag{17}$$

Finally, the electric field of the laser light at the interface is the sum of the incident and reflected fields.[46]

$$E_{int} = \begin{pmatrix} (1+r_{||})(A\exp(i\phi)\cos\beta - B\sin\beta) \\ -(1+r_{\perp})(A\exp(i\phi)\sin\beta\cos\chi + B\cos\beta\cos\chi) \\ (1-r_{\perp})(A\exp(i\phi)\sin\beta\sin\chi + B\cos\beta\sin\chi) \end{pmatrix}_{xyz} \tag{18}$$

The orientation of the transition dipole is described by the angles ξ and φ in Figure 4. The adsorption intensity can be described as[47]

$$I_{abs,i} = D\int_0^{\pi}\int_0^{2\pi} f(\xi,\varphi)|M_i|^2\,d\varphi\,d\xi \tag{19}$$

where i stands for the coordinates (x,y,z), $f(\xi,\varphi)$ is the distribution function of the angles ξ and φ, and D is a constant proportional to the density of transition moments. Considering a Dirac distribution of the orientation angle ξ and a uniform distribution of φ around the normal to the interface (z axis), the following expression is obtained for the absorption intensity:[47,48]

$$I_{abs} = \begin{pmatrix} D\pi\sin^2\xi \\ D\pi\sin^2\xi \\ 2D\pi\cos^2\xi \end{pmatrix} \tag{20}$$

It should be noted that, for an orientation angle of 45°, the absorption intensity given by eq 20 is the same as what would be obtained with a random distribution of the angle ξ. Since the angles measured in the presence of porphyrins are above 50° in

(46) Chabal, Y. J. *Surf. Sci. Rep.* **1988**, *8*, 211.
(47) Akutsu, H.; Kyogoku, Y.; Nakahara, H.; Fukuda, K. *Chem. Phys. Lipids* **1975**, *15*, 222.
(48) Ohta, N.; Matsunami, S.; Okazaki, S.; Yamazaki, I. *Langmuir* **1994**, *10*, 3909.

most cases, we can exclude that there is no specific orientation of the porphyrin rings. However, the distribution is probably more adequately described with a Gaussian function. Such a distribution can be easily introduced into eq 19. In the following analysis, we shall restrain ourselves to single ξ values since we lack any information on the possible width of the ξ distribution. Although this situation might introduce errors in the evaluation of the orientation angle, we believe that the trends observed in the dependence of the porphyrin orientation on the concentration and potential remain valid. The intensity of the detector signal can be written as

$$I = I_0 - P(|E_{\mathrm{int},x}|^2 I_{\mathrm{abs},x} + |E_{\mathrm{int},y}|^2 I_{\mathrm{abs},y} + |E_{\mathrm{int},z}|^2 I_{\mathrm{abs},z}) \quad (21)$$

where P is a proportionality constant depending on the characteristics of the photomultiplier tube. To allow comparison between responses at various light intensities, the reflectance is expressed as

$$\Delta R = \frac{I - I_0}{I_0} \quad (22)$$

To simplify the expression, the various scaling factors are grouped into a single constant

$$C = E_0 DP \quad (23)$$

The solid lines in Figures 3 and 8 are fits to eq 22 employing C and ξ as adjustable parameters.

LA052642B